Supplementary Information – Molecular Pharmacology

Identification of determinants required for agonistic and inverse agonistic ligand properties at the ADP receptor $P2Y_{12}$

Philipp Schmidt, Lars Ritscher, Elizabeth N. Dong, Thomas Hermsdorf, Maxi Cöster, Doreen Wittkopf, Jens Meiler and Torsten Schöneberg

Molecular Biochemistry, Institute of Biochemistry, Medical Faculty, University of Leipzig, 04103 Leipzig, Germany (P.S., L.R., T.H., M.C., D.W., T.S.). Center for Structural Biology, Vanderbilt University Medical Center, Nashville, TN, USA (E.N.D., J.M.). Department of Pharmacology, Vanderbilt Program in Drug Discovery, Vanderbilt University Medical Center, Nashville, TN, USA (J.M.). Department of Chemistry and the Institute for Chemical Biology, Vanderbilt University Medical Center, Nashville, TN, USA (J.M.).

Figure S1

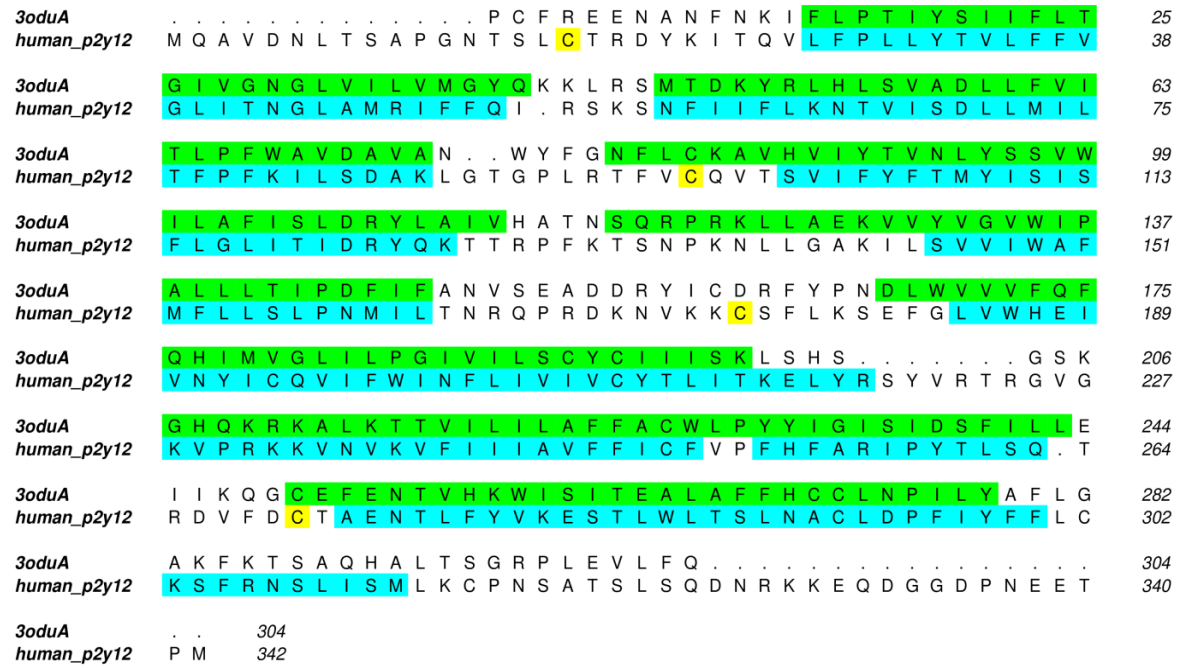

Suppl. Figure S1. **Sequence alignment of $P2Y_{12}$ with CXCR4.**

The sequence of human $P2Y_{12}$ was aligned with the sequence of human CXCR4 (PDB ID: 3ODU) (Gupta et al., 2001) using CLUSTALW (Larkin et al., 2007). Transmembrane helical regions of the CXCR4 receptor are highlighted in green. Regions predicted to be transmembrane helical regions of $P2Y_{12}$ according to secondary structure prediction server PSIPRED (McGuffin et al., 2000) are highlighted in cyan. Cysteine residues known to form disulphide bonds are highlighted in yellow.

Figure S2

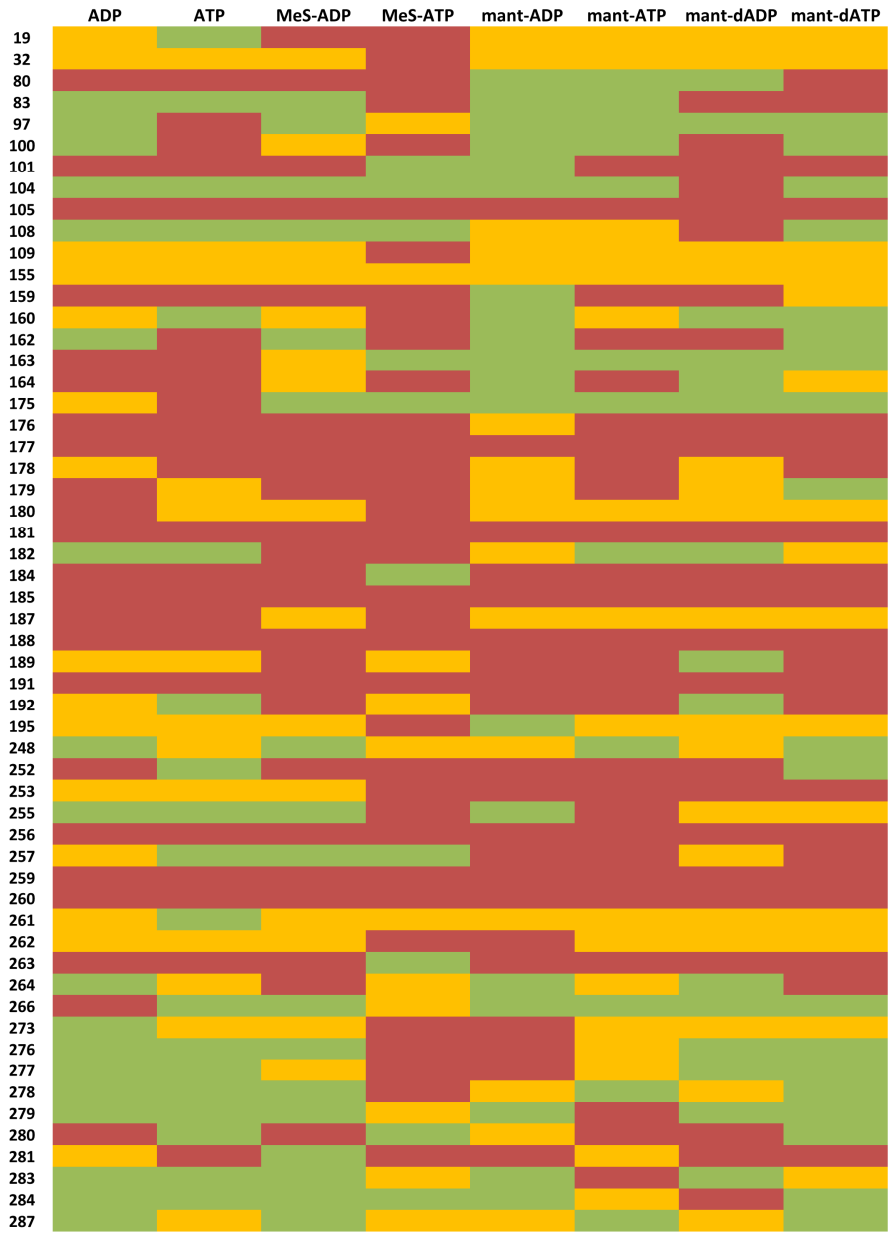

Suppl. Figure S2. **Per residue change in free energy with and without ATP derivatives bound.**

Rosetta was used to determine the difference in change in free energy (ΔΔG) between $P2Y_{12}$ with and without ATP derivatives bound. Residues that demonstrated the largest difference in free energy change in respect to bound ADP, ATP, MeS-ADP, MeS-ATP, mant-ATP, mant-ADP, mant-dADP and mant-dATP are listed. For each ligand, residues with ΔΔG above the average energy change (-0.24) are in red, while those with energy change above average but still negative are in yellow and residues with a positive energy change are in green.

Figure S3

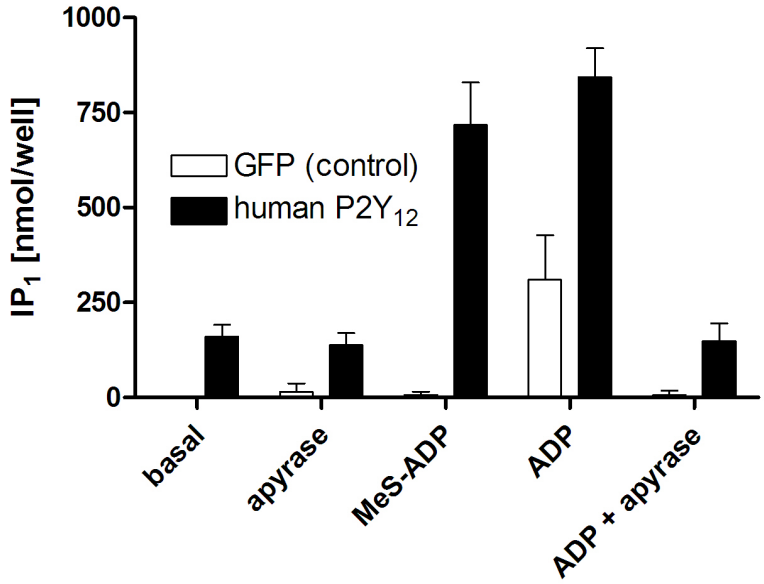

Suppl. Figure S3. **Analysis of the functional impact of endogenous nucleotide released from CHO cells**

To analyze of whether endogenous nucleotide released from CHO cells contribute to basal activity of $P2Y_{12}$ we performed control experiments with CHO-K1 cells stably transfected with $G\alpha_{qi4}$. Intracellular inositol phosphate (IP_1) levels were determined with an immunological assay (cisbio Bioassays, IP-One ELISA, part-no. 72IP1PEA).

$G\alpha_{qi4}$-CHO-K1 cells transiently transfected with $P2Y_{12}$ presented an increased basal IP_1 level compared to cells transfected with the control plasmid (GFP). Incubation with 12.5 U/ml apyrase did not reduce this elevated IP_1 level. This clearly indicates that $P2Y_{12}$ does induce signal transduction by intrinsic active receptor conformation and not by nucleotides released from the cells into the medium. Proper $P2Y_{12}$ transfection was control by application of 100 µM ADP and 100 µM MeS-ADP. Proper apyrase function was demonstrated by loss of ADP action on $P2Y_{12}$.

Table

Suppl. Table S1. **Purine compound library screening at the human WT $P2Y_{12}$**

The activity of compounds (given in %) at the human $P2Y_{12}$ expressed in yeast is shown relative to the basal activity ($OD_{600\ nm}$ =0.089; set 0%) and the stimulation with 10 µM MeS-ADP ($OD_{600\ nm}$ =0.667; set 100%). Stimulation was measured after 24 h with 10 µM of the respective compound.

AMP -2.19	ADP 84.05	ATP 19.93	AP4 -0.29	cAMP -0.99
3'-dATP -2.02	7-Deaza-dAMP -1.33	NPE-caged-ATP -0.64	7-Deaza-dATP -1.33	DMB-caged-ATP 5.24
dATPαS -1.68	ADPβS 92	ATPγS 71.09	β-Methylene-APS -1.68	ApCp -0.81
AP3A -0.99	AP4A -1.5	AP5A -1.68	AP6A -1.68	AP4U -0.99
AP4(8I)G -2.37	AP5(8I)G -1.68	2'I-AMP -1.33	2'I-ADP -1.68	2'I-ATP -1.16
8Br-ADP 0.57	8Br-ATP -1.68	8Br-dATP -0.99	γ-[6-Aminohexyl]-ATP -1.5	2I-ATPγS 90.1
7-Deaza-7Br-dATP -2.02	γ-Aminophenyl-ATP 2.99	γ-[(6-Aminohexyl)-imido]-ATP -1.16	γ-[(8-Aminooctyl)-imido]-ATP -1.16	N6-(4-Amino)butyl-ATP -1.33
EDA-ATP -3.75	γ-[6-Aminohexyl]-N6-Benzyl-ATP -2.02	2-Hydroxy-ATP -1.5	TNP-ADP 72.81	TNP-ATP 4.03
1-Methyl-AMP -0.99	1-Methyl-ADP 1.61	1-Methyl-ATP 0.05	dATP 0.57	ddATP 0.57
2'.5'-pAp -0.47	ara-ATP 0.4	AMPαS -0.12	ATPαS 2.3	dADPαS 0.4
ApCpp -1.33	AppCp 0.4	dApCpp -0.47	AppNp 0.57	AppNH2 76.79
AP5U -1.16	AP4T -0.29	AP5T -0.47	AP4G 0.22	AP5G 0.05
2'Br-ADP -1.16	2'Br-ATP -0.64	2'-Ome-ATP -0.81	mante-ATPγS -0.4	8Br-cAMP 0.05
2'F-AMP -0.81	2'F-ATP -0.47	2'Cl-ATP -0.81	BzBzATP -0.12	7-Deaza-7I-dATP -0.12
N6-(6-Amino)hexyl-ATP -0.81	N6-(6-Amino)hexyl-dATP -0.12	8-[(4-Amino)butyl]-amino-ATP -0.12	8-[(6-Amino)hexyl]-amino-ATP 0.57	EDA-ADP 1.95
mant-ADP 6.79	mant-ATP -0.47	mant-dATP -0.64	mant-N6-Methyl-ATP -0.29	ε-ATP 0.4
Adenine 0.6	Adenosine 0.75	IMP 0.15	UDP 2.54	Xanthine 0.75
GDP 1.94	GTP 0.75	GTPγS 0.45		